

Diffusion in the Continuous-Imaginary-Time Quantum World-Line Monte Carlo Simulations with Extended Ensembles

Kenji HARADA and Yuto KUGE

Graduate School of Informatics, Kyoto University, Kyoto 606-8501

The dynamics of samples in the continuous-imaginary-time quantum world-line Monte Carlo simulations with extended ensembles are investigated. In the case of a conventional flat ensemble on the one-dimensional quantum $S = 1$ bi-quadratic model, the asymmetric behavior of Monte Carlo samples appears in the diffusion process in the space of the number of vertices. We prove that a local diffusivity is asymptotically proportional to the number of vertices, and we demonstrate the asymmetric behavior in the flat ensemble case. On the basis of the asymptotic form, we propose the weight of an optimal ensemble as $1/\sqrt{n}$, where n denotes the number of vertices in a sample. It is shown that the asymmetric behavior completely vanishes in the case of the proposed ensemble on the one-dimensional quantum $S = 1$ bi-quadratic model.

KEYWORDS: diffusion, extended ensemble, quantum Monte Carlo, first-passage time, bi-quadratic model

Properties of various quantum exotic states and phase transitions between them have been extensively investigated. For example, quantum paramagnetic and valence-bond-solid states related to a possible mechanism to support a novel superconductivity in cuprates,¹⁾ and the existence of non-Landau-Ginzburg-Wilson type phase transitions between different broken symmetries.²⁾ In order to numerically investigate such quantum states and phenomena, unbiased quantum world-line Monte Carlo (QMC) methods based on a Markov chain are powerful tools, because they can be applied to large scale systems at low temperatures and are not limited to the one-dimensional case, if no negative-sign problem exists. However, even for no negative-sign cases, it is sometimes difficult to get accurate data from the conventional QMC simulations, because Monte Carlo samples are trapped near a metastable state in configuration space. In general, the quality of QMC simulations deteriorates at low temperatures, because metastable states are related to degenerate ground states. In fact, the autocorrelation time of samples in QMC simulations becomes exponentially large to overcome barriers between metastable states. In order to eliminate the rapid increase in autocorrelation times in Monte Carlo simulations, two approaches were proposed over the last two decades. One is to change the local update method of samples in a Markov process to a global one that connects metastable states directly. In fact, the loop algorithm³⁾ has been successful in studies of quantum magnetic phases due to the global update whose shape is like a loop and which corresponds to a magnetic correlated domain. However, in some cases using the loop algorithm, we encountered rapid increases in autocorrelation time: For example, valence-bond-solid states that break spatial symmetries on the two and quasi-one dimensional lattice.^{4,5)} For such cases, the second approach is probably effective, in which a canonical ensemble is replaced by an artificial extended ensemble such that Monte Carlo samples would not be trapped near metastable states. For classical systems, the extended weight is adjusted such that the appearance ratio

of energy E samples would be flat. They are not trapped near a metastable state because Monte Carlo samples diffuse in a wide energy range. Therefore, these methods have been extensively used for studies of spin glasses and frustrated classical models. However, for quantum models, they have been tested only in a few cases.^{6,7)} In order to get conclusive numerical results for quantum strong correlated phenomena as mentioned above, we need to understand the property of QMC methods with extended ensembles, and it is important to improve their efficiencies. In this letter, we will concentrate the diffusive behavior of samples in the continuous-imaginary-time QMC simulations with an extended ensemble. We will report the asymmetric behavior in the diffusion process for the one-dimensional quantum $S = 1$ bi-quadratic (BQ) model case. On the basis of our proven asymptotic form of the local diffusivity of samples, we will propose an optimal ensemble. The performance of the proposed ensemble will be shown for the case of the one-dimensional BQ model.

Although the first formulation of QMC methods with extended ensembles (EEQMC) was based on high-temperature series expansion,⁶⁾ it can be also done on the path-integral representation with a continuous-imaginary-time limit (see §2.15 in ref. 8). In order to provide a brief description of the EEQMC algorithms on the path-integral representation, we first consider the definition of the exponential operator:

$$\exp\left(-\beta \sum_b \mathcal{H}_b\right) = \lim_{M \rightarrow \infty} \left[\prod_b \left(1 - \frac{\beta \mathcal{H}_b}{M}\right) \right]^M. \quad (1)$$

Inserting the identity operator $1 = \sum_\alpha |\alpha\rangle\langle\alpha|$ with a complete orthonormal basis $\{|\alpha\rangle\}$ between two adjacent factors in the right-hand side of eq. (1), we obtain the discrete-imaginary-time path-integral representation of a partition function as

$$Z \approx \sum_{\{|S_b(t)\rangle\}} \prod_{t=1}^M \prod_{b=1}^K \langle S_{b+1}(t) | (1 - \beta \mathcal{H}_b \Delta) | S_b(t) \rangle, \quad (2)$$

where \mathcal{H}_b is the b -th interaction Hamiltonian, β is an inverse temperature, $\Delta = 1/M$, $S_{K+1}(t) \equiv S_1(t+1)$, and $S_1(M+1) \equiv S_1(1)$. Next, we introduce new auxiliary variables $G_b(t)$ called *graph variables* as $(1 - \beta\mathcal{H}_b\Delta) = \sum_{G_b(t)=0,1} (-\beta\mathcal{H}_b\Delta)^{G_b(t)}$. Then, eq. (2) is rewritten as

$$Z \approx \sum_S \sum_G \beta^{n(G)} W_0(S, G) = \sum_n \beta^n \Omega(n), \quad (3)$$

$$W_0(S, G) = \prod_u \langle S_{u'} | (-\mathcal{H}_u \Delta)^{G_u} | S_u \rangle, \quad (4)$$

$$\Omega(n) = \sum_S \sum_{G|n(G)=n} W_0(S, G), \quad (5)$$

where u , u' , S , and G denote (b, t) , $(b+1, t)$, $\{S_u\}$, and $\{G_u\}$, respectively, and $n(G) = \sum_u G_u$. In the following, a graph variable G_u that takes a value 1 is called a *vertex* and the number of vertices $n(G)$ is called a *vertex number*. This representation is the mathematical background required to describe the remarkable QMC algorithms that have been developed during the last two decades.⁸⁾ In particular, we can take a limit of a continuous-imaginary time, $\Delta \rightarrow 0$, in the level of QMC algorithms (see §2.5 in ref. 8 for details). In the remainder of this paper, we consider the EEQMC algorithm on the continuous-imaginary time, because it has no systematic error from the discretization of an imaginary time.

The vertex number $n(G)$ in a canonical ensemble statistically corresponds to an inverse temperature β because $\langle n(G) \rangle_\beta = \beta \langle -\mathcal{H} \rangle_\beta$, where $\langle \cdot \rangle_\beta$ is a canonical ensemble average. Therefore, if we adjust the weight of a configuration (S, G) so that the frequency of obtaining the vertex number n would be independent of n , i.e., flat,⁶⁾ we can sample various configurations in a wide inverse temperature range. From eq. (3), $\Omega(n)$ is regarded as the density of states with a fixed vertex number n . Hence, if the factor $\beta^{n(G)}$ in eq. (3) is replaced by $1/\Omega(n(G))$, it can be done. In general, in order that the appearance ratio of configurations with a vertex number n is $P_v(n)$, the extended ensemble weight of a configuration (S, G) has to be $P_v(n(G))W_0(S, G)/\Omega(n(G))$. However, we need to guess $\Omega(n)$ from the QMC samples themselves, because $\Omega(n)$ is not known a priori. Fortunately, some sophisticated methods have been proposed.^{9,10)} In our simulations, we have used the broad-histogram relation for the vertex number¹¹⁾ as

$$\frac{\Omega(n+1)}{\Omega(n)} = \frac{\langle \text{diag}(-\mathcal{H}) \rangle_n}{n+1 - \langle n_K \rangle_{n+1}}, \quad (6)$$

where $\langle Q \rangle_n$ denotes the micro-canonical ensemble average of an operator Q at a fixed vertex number n , $\text{diag}(Q)$ refers to the diagonal part of an operator Q , and n_K is the number of kinks at which a state changes, i.e., $\langle S_{u'} | S_u \rangle = 0$. Because the right-hand side in eq. (6) can be directly estimated in the EEQMC simulations, $\Omega(n)$ can be calculated from this recursion formula. We should note that this estimation method is independent of the dynamics of the EEQMC samples; it is not based on the histogram of the appearance of a vertex number in the EEQMC simulations.

However, after $\Omega(n)$ is sufficiently estimated, the dy-

namics of the EEQMC samples do not seem to be a regular random walk in the vertex number space. In particular, in order to investigate this behavior, we focus on the first-passage time (FPT) of EEQMC samples regarded as random walkers in a vertex number space. The FPT is defined as the time at which a random walker first reaches a threshold value. Because the movement of an EEQMC sample is usually restricted to the interval $[N_a, N_b]$ in the vertex number space, two types of FPTs are defined as a QMC sample moves to N_b from N_a , and vice versa. In the following, the former is called *forward* and the latter is called *backward*.

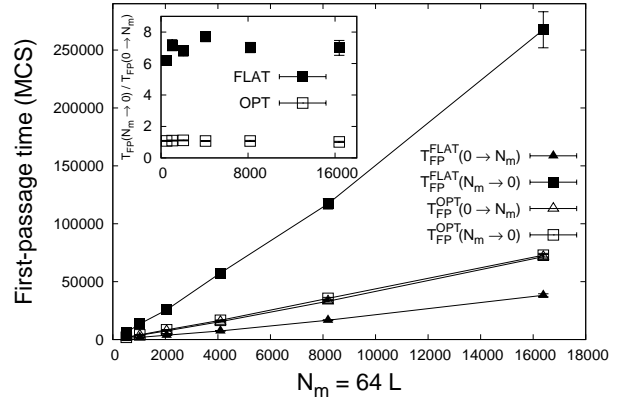


Fig. 1. First-passage times (FPT) of EEQMC samples for the one-dimensional quantum $S = 1$ bi-quadratic model. Filled triangle and square symbols are forward and backward FPTs for a flat ensemble, respectively. Triangle and square symbols are forward and backward FPTs for the ensemble defined by eq. (15), respectively. In the inset, the ratios of backward and forward FPTs are shown.

Figure 1 shows forward and backward FPTs, $T_{\text{FP}}(0 \rightarrow N_m)$ and $T_{\text{FP}}(N_m \rightarrow 0)$, for the one-dimensional BQ model with chain lengths $L = 8, 16, 32, 64, 128$, and 256. The Hamiltonian of the BQ model on the one-dimensional lattice is $\mathcal{H} = -\sum_i (\mathbf{S}_i \cdot \mathbf{S}_{i+1})^2$, where \mathbf{S}_i denotes an $S = 1$ spin operator at the i -th site. Because this model is integrable, the ground state is well known as the dimerized state in which singlet pairs align and completely cover the one-dimensional lattice. This dimerized state is twofold degenerate and spontaneously breaks a translational symmetry. And the autocorrelation time in QMC simulations is the round-trip time between such degenerate states. As mentioned above, even if we use a loop algorithm for the BQ model,¹²⁾ it grows rapidly at low temperatures. Therefore, this model is suited to the test of the EEQMC algorithms. In all cases, N_m is proportional to the chain length L as $N_m = 64L$. It corresponds to a constant low temperature enough to calculate a ground state, because the one-dimensional BQ model has a gap. The total number of EEQMC samples for a chain length is sufficiently large for estimating FPTs: For example, 32 independent runs with 6×10^6 Monte Carlo sweeps (MCSs) for $L = 256$. We should note that MCS is adopted as a unit of time. One MCS for a configuration (S, G) in the continuous-imaginary-time

EEQMC algorithm consists of three steps: (i) deciding a new vertex number n' under a given S -configuration, (ii) assigning new graphs G' with the vertex number n' to a given S -configuration, and (iii) choosing a new S' -configuration under the given graphs G' . It is possible to measure observables only at the time that these three steps are completed. In Fig. 1, forward and backward FPTs for a flat ensemble increase almost linearly, but the backward FPT is always larger than the forward one: For example, the ratio of two FPTs is 7.0(5) for $L = 256$ (see the inset of Fig. 1). Thus, the EEQMC samples for a flat ensemble move quickly from high temperatures to low ones, but slowly in the reverse direction. In order to improve the efficiency of the EEQMC algorithms, it is necessary to correct this asymmetric behavior.

When we make a new G' configuration under a fixed S -configuration, the vertex ($G_u = 1$) at a kink can not be removed, because the local weights in $W_0(S, G)$ at a kink becomes zero: $\langle S_{u'} | S_u \rangle = 0$. Therefore, if the number of kinks is n_K , the probability $p(n' | n_K)$ to choose the next vertex number n' in step (i) is proportional to the sum of weights of the configurations that have unchanged n_K vertices at kinks and new inserted $(n' - n_K)$ ones into a given S -configuration:

$$p(n' | n_K) \propto \frac{P_v(n') \left[\sum_{(u|G_u=0)} \langle S_{u'} | (-\mathcal{H}_u \Delta) | S_u \rangle \right]^{(n'-n_K)}}{\Omega(n')(n' - n_K)!}. \quad (7)$$

For finite-size systems, if the vertex number is sufficiently large, the right-hand side in eq. (6) is converged. Using limiting values as $w_0 = \lim_{n \rightarrow \infty} \langle \text{diag}(-\mathcal{H}) \rangle_n$ and $r_K = \lim_{n \rightarrow \infty} \langle n_K \rangle_n / n$, the asymptotic form of $\Omega(n)$ is as

$$\Omega(n) \approx \frac{\Omega(n-1)}{n} \left(\frac{w_0}{1-r_K} \right) \propto \frac{1}{n!} \left(\frac{w_0}{1-r_K} \right)^n. \quad (8)$$

Substituting eq. (8) into eq. (7), we find that the main factor of $p(n' | n_K)$ is the negative binomial distribution. Using the limit theorem for the negative binomial distribution, we obtain the asymptotic form of $p(n' | n_K) \propto P_v(n') \exp[-(n' - m_0)^2 / 2(m_0 / r_K)]$, where $m_0 \equiv (r_K^{-1} - 1)n_K$. Here, we assume that $P_v(n')$ is a slowly varying function. And if we assume that the probability $p(n_K | n)$ that the number of kinks in a configuration with a vertex number n is n_K is equivalent to the probability $p(n | n_K)$, the probability to choose the next vertex number n' from configurations with a vertex number n is

$$p(n \rightarrow n') = \int_0^n dn_K p(n' | n_K) p(n_K | n), \quad (9)$$

$$\approx N_G \left(n, \left[\frac{2(1-r_K)}{r_K} \right] n \right), \quad (10)$$

where $N_G(m, \sigma^2)$ denotes the Gaussian distribution with mean m and variance σ^2 . Thus, the EEQMC samples almost seem to be random walkers in the vertex number space, but the local diffusivity $D(n)$ increases linearly as

$$D(n) \approx \left[\frac{(1-r_K)}{r_K} \right] n, \quad (11)$$

where n is the number of vertices in a configuration. Fig-

ure 2 shows the local diffusivity $D(n)$ for a flat ensemble ($P_v(n) = 1$) in the EEQMC simulations of the one-dimensional BQ model. The chain length L is 128 and the total number of MCSs is 1.05×10^8 . The local diffusivity in Fig. 2 is approximately linear in the region above the vertex number 100 (see also the left-top inset of Fig. 2). The solid line in Fig. 2 is a linear function predicted in eq. (11) with $r_K = 0.6108(1)$, which is evaluated from the QMC simulations. The predicted line is consistent with the local diffusivity in the region above the vertex number 1000. And the discrepancy between them is never more than 6% at all vertex numbers below 1000 but zero. Next, we checked the dependence of the local diffusivity on extended ensembles. In the right-bottom inset of Fig. 2, the ratios between local diffusivities in two different ensembles are shown. Because these values are approximately equal to one, the local diffusivity is almost unaffected by the choice of extended ensembles. For other system-size cases, the same results were obtained. Therefore, the local diffusivity of the EEQMC samples is described well by eq. (11).

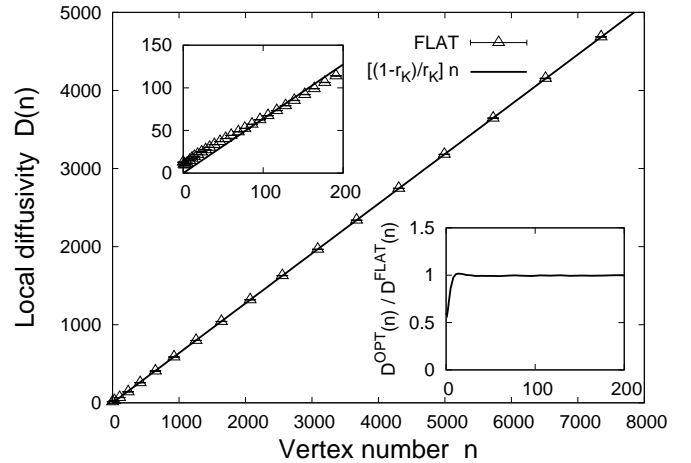


Fig. 2. Local diffusivity in the EEQMC simulations of the one-dimensional quantum $S = 1$ bi-quadratic model. The chain length L is 128. The extended ensemble is flat: $P_v(n) = 1$. The solid line shows the predicted linear increase in eq. (11). The value of r_K is 0.6108(1), which is evaluated from the QMC simulations. In the left-top inset, the local diffusivity in the small vertex number region is shown. In the right-bottom inset, the ratios between local diffusivities in a flat ensemble and the optimal one defined by eq. (15) are shown.

From eq. (10), the behavior of the samples in the EEQMC simulations may be described well by a Fokker-Planck equation (FPE) on a vertex number range $[N_a, N_b]$.¹³⁾ Using the theory of first-passage processes,¹⁴⁾ we can explicitly obtain the first-passage times for a one-dimensional FPE as

$$T_{\text{FP}}(N_a \rightarrow n) = \int_{N_a}^n dx P_v(x) \int_x^n \frac{dx'}{D(x')P_v(x')}, \quad (12)$$

$$T_{\text{FP}}(N_b \rightarrow n) = \int_n^{N_b} dx P_v(x) \int_n^x \frac{dx'}{D(x')P_v(x')}. \quad (13)$$

If we assume the linear increase of the local diffusivity

$D(n)$ as in eq. (11), FPTs for a flat ensemble ($P_v(n) = 1$) are as

$$T_{\text{FP}}^{\text{FLAT}}(0 \rightarrow N_m) \approx \frac{N_m}{r_K^{-1} - 1}, \quad \frac{T_{\text{FP}}^{\text{FLAT}}(N_m \rightarrow 0)}{T_{\text{FP}}^{\text{FLAT}}(0 \rightarrow N_m)} \approx \log N_m. \quad (14)$$

These results are qualitatively consistent with the behavior of FPTs in Fig. 1. The forward FPT increases linearly and the backward one is always larger than the forward one and their ratio varies slowly. Thus, the qualitative behavior of the EEQMC samples is described well by the FPE with eq. (11).

In order to correct the asymmetry between forward and backward FPTs for a flat ensemble, an extended ensemble $P_v(n)$ should be adjusted so that the right-hand side in eq. (12) would be equivalent to that in eq. (13). While it typically cannot be uniquely determined, a special solution exists: $P_v(n) = 1/\sqrt{D(n)}$. This special ensemble was first derived from a maximization of random walker flows.¹⁵⁾ Using this ensemble, we find that the forward FPT is not only equivalent to the backward one, but also the total FPT, $T_{\text{FP}}(0 \rightarrow N_m) + T_{\text{FP}}(N_m \rightarrow 0)$, is minimized.¹³⁾ Therefore, from eq. (11), the optimal ensemble for the EEQMC methods is

$$P_v^{\text{OPT}}(n) = \frac{1}{\sqrt{D(n)}} \propto \frac{1}{\sqrt{n}}. \quad (15)$$

Substituting eqs. (11) and (15) into eqs. (12) and (13), we find that the forward and backward FPTs for the optimal ensemble are equivalent and become twice as large as the forward one for a flat ensemble:

$$T_{\text{FP}}^{\text{OPT}}(N_m \rightarrow 0) = T_{\text{FP}}^{\text{OPT}}(0 \rightarrow N_m) = 2T_{\text{FP}}^{\text{FLAT}}(0 \rightarrow N_m). \quad (16)$$

The forward and backward FPTs in the EEQMC simulations with the optimal ensemble are shown in Fig. 1. Here, although eq. (11) is the asymptotic form, we use eq. (15) for all vertex numbers except zero, and the value at the vertex number zero is defined by that at the vertex number one: $P_v(0) \equiv P_v(1)$. In Fig. 1, the forward FPT for our proposed ensemble is consistent with the backward one (see also the inset of Fig. 1). And, as in eq. (16), they are approximately twice as large as the forward FPT for a flat ensemble. Thus, the asymmetry is completely corrected by the ensemble in eq. (15).

As mentioned above, we adopt MCS as the unit of time. But the actual computational times for one MCS are not constant. In fact, in many cases the number of local steps in one MCS is proportional to the vertex number in a sample. Therefore, the local step can be adopted as the unit of time. In this case, from eq. (11), we find that the local diffusivity in units of local steps is independent of the vertex number. Hence, the optimal ensemble in units of local steps is flat. In other words, the optimal ensemble for computational times is as $P_v^{\text{LOPT}}(n) = 1/n$. The total local steps of FPTs is $\frac{3}{4}$ times that for P_v^{OPT} . But the number of samples in the region of large vertex numbers decreases more than that for P_v^{OPT} . In order to calculate a canonical ensemble average of an observable at an inverse temperature β , it is necessary to calculate

the reweighted summation of micro-canonical ensemble averages. Vertex numbers that mainly contribute to it are in the region of which the width is proportional to $\sqrt{n(\beta)}$, where $n(\beta)$ is a center of the region. Therefore, in the case of P_v^{OPT} , the number of samples that contribute to a canonical ensemble average is constant at all inverse temperatures. But that for the ensemble P_v^{LOPT} decreases at low temperatures.

In summary, we considered the diffusion of samples in the continuous-imaginary-time EEQMC simulations. In particular, the asymmetric behavior of FPTs of EEQMC samples was reported in detail. We proved that the local diffusivity of the EEQMC samples is asymptotically proportional to the vertex number. And it was shown that the asymptotic form is consistent with the local diffusivity in the EEQMC simulations of the one-dimensional BQ model in the wide region of the vertex numbers. Using this result and the theory of first-passage processes, we demonstrated the asymmetric behavior of FPTs for a flat ensemble case and proposed an optimal ensemble for the continuous-imaginary-time EEQMC simulations in order to correct the asymmetric behavior. It was shown that the asymmetric behavior on the one-dimensional BQ model completely vanishes in the case of the proposed ensemble.

The author would like to thank Naoki Kawashima for useful comments. The computation in the present work is executed on computers at the Supercomputer Center, Institute for Solid State Physics, University of Tokyo. The present work is financially supported by MEXT Grant-in-Aid for Scientific Research Wakate (B) 19740237 (2007) and Kiban (B) 19340109 (2007) and by Next Generation Supercomputing Project, Nanoscience Program, MEXT, Japan.

- 1) P. W. Anderson: *Science* **235** (1987) 1196.
- 2) T. Senthil, A. Vishwanath, L. Balents, S. Sachdev, and M. P. A. Fisher: *Science* **303** (2004) 1490.
- 3) H. G. Evertz, G. Lana, and M. Marcu: *Phys. Rev. Lett.* **70** (1993) 875; H. G. Evertz: *Advances in Physics* **52** (2003) 1.
- 4) K. Harada, N. Kawashima, and M. Troyer: *Phys. Rev. Lett.* **90** (2003) 117203.
- 5) K. Harada, N. Kawashima, and M. Troyer: *J. Phys. Soc. Jpn.* **76** (2007) 013703.
- 6) M. Troyer, S. Wessel, and F. Alet: *Phys. Rev. Lett.* **90** (2003) 120201.
- 7) S. Wessel, N. Stoop, E. Gull, S. Trebst, and M. Troyer: *J. Stat. Mech.* (2007) P12005.
- 8) N. Kawashima and K. Harada: *J. Phys. Soc. Jpn.* **73** (2004) 1379.
- 9) F. Wang and D. P. Landau: *Phys. Rev. Lett.* **86** (2001) 2050.
- 10) P. M. C. de Oliveira, T. J. P. Penna, and H. J. Herrmann: *Eur. Phys. J. B* **1** (1998) 205.
- 11) C. Yamaguchi, N. Kawashima, and Y. Okabe: *J. Phys. Soc. Jpn.* **73** (2004) 1728.
- 12) K. Harada and N. Kawashima: *J. Phys. Soc. Jpn.* **70** (2001) 13.
- 13) W. Nadler and U. H. E. Hansmann: *Phys. Rev. E* **75** (2007) 026109.
- 14) S. Redner: *A Guide to First-Passage Processes* (Cambridge University Press, Cambridge, 2001), p. 38.
- 15) S. Trebst, D. A. Huse, and M. Troyer: *Phys. Rev. E* **70** (2004) 046701.